

# Electric Karting Modeling Using Induction Motor in Matlab<sup>®</sup>/Simulink<sup>®</sup> Software

Didi Istardi

\* Batam Polytechnics

Parkway, Batam Centre, Batam, 29461, Indonesia

E-mail: istardi@polibatam.ac.id

**Abstract**—An electric traction motor drive for an electric karting application was modeled for efficiency studies and simulated using the MATLAB<sup>®</sup>/Simulink<sup>®</sup> software. The model includes models of a battery, power electronic converter, electric motor, and vehicles dynamic of go-karts to a typical 48 seconds track driving schedule. The losses of each component of the electric traction motor drive were modeled and simulated over the entire speed range. In the battery was also calculated the state of charge (SOC) of the battery over the driving cycle. The regenerative braking energy captured was also considered in the simulation. Finally, the overall electric traction motor drive system efficiency and energy consumed were estimated based on the individual model based efficiency and energy consumed analysis.

**Index Terms**—Battery, electric go-kart, efficiency maps, loss modeling, and regenerative braking.

## I. INTRODUCTION

The first electric vehicle was made in the 1830s and was popular for almost a century [1],[2],[3]. However, since 1933 the numbers of electric vehicles have decreased due to the improvements of the internal combustion engine (ICE) that has become better and cheaper. Nowadays, environmental considerations, energy costs, and improvements in control and battery technology have inspired an increasing amount of research and development of electric vehicles [3].

One of the developments in the electric vehicle is research on electric kart racing or karting. Research in this area is interesting due to their characteristics that were different compare to the normal electric go-kart such as energy consumption. In electric karting, the electric karting is higher than in the electric go-kart. The drive cycle that was used in the electric karting have a high acceleration and deceleration. In this paper, the electric karting that would be used as a input for simulation is the ICE karting for children (8-12 years old) because it is easier to introduce a new concept to children compare to adult. Therefore, the research is focus on energy consumption and losses of an electric micro karting.

Electric karting is a variant of an open-wheel motor sport,

with small four-wheeled vehicles called karts. These karts are simple and usually raced on a scaled-down track. Since the electric kart engine is powered by an electric motor instead of an internal combustion engine and the motor is operated using the power stored in batteries [4], its engine has many advantages over the ICE. It is pollution-free, has higher energy conversion efficiency and less vibration, requires low maintenance, its speed is easy to control and it can use the energy from regenerative braking [1], [3]. An electric karting race was first started in 1989 in Italy [5] and is currently getting popular in the United States and Europe due to improvements in control and battery technology.

The components of electric karting are chassis made of a steel tube, a propulsion system that includes an electric motor that drives the wheels, a power electronic converter that regulates the energy flow to the motor and a transmission system, a battery that provides energy, and a control unit that ensures a proper operation of the power electronic converter [3],[6], [7].

The paper is organized as follows: In the next section, a brief review of electric traction drive system components and simulation of each component are presented. In Section III, a description of the ICE karting drive cycle is given. Section IV and V presents results of simulation using MATLAB<sup>®</sup>/Simulink<sup>®</sup> software and discussion of the results. Finally, the conclusions are made in section VI.

## II. ELECTRIC TRACTION DRIVE SYSTEM

A simple electric traction drive system consists of a drive system (transmission, electric motor, and power electronics) and energy storage (battery) [6] as seen in Fig. 1. Examples of some papers that describe the modeling of an electric traction drive system using MATLAB<sup>®</sup> or other software [7]-[10].

Within the system, energy is stored in the battery. A power electronic converter connects the battery to an electric motor. The voltage and current output of the battery are maintained to match the ratings of the electric motor. The electric motor converts electrical energy supplied by the battery into mechanical energy. A transmission transforms the mechanical energy into a linear motion. Speed and torque are adjusted using the gear box. The gear can transmit the rotational force at

---

Didi Istardi is with Batam Polytechnics Lecturer (e-mail: istardi@polibatam.ac.id).

Telp : +62-778-469856 ext 1071

Fax : +62-778-463620

different speeds, torque, and directions. A controller and energy management control the speed and direction of the electric karting, and optimize the energy conversion from the battery to the transmission. The battery can be charged from the line power and also from regenerative braking energy.

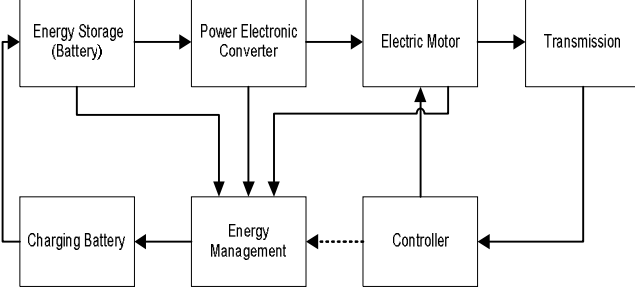


Fig. 1. Block diagram of drive system for electric karting.

In order to calculate the efficiency of the electric karting, it is essential to understand how the losses of each electric drive system component change with speed.

#### A. Vehicle Dynamic Model

Mechanical energy provided by the electric traction drive system is used to drive the wheels of the electric karting. The supplied energy must be large enough to overcome the “traction resistance” ( $F_t$ ), i.e. the sum of rolling resistance ( $F_{rr}$ ), aerodynamic drag ( $F_{ad}$ ), climbing resistance and acceleration force ( $F_{af}$ ) [8], [11]. Rolling resistance is a deformation process mechanism which occurs at the contact patch between the tires and road surface. Aerodynamic drag is the viscous resistance of air upon the vehicle. In this paper, the race track is assumed to be flat, thus the climbing resistance is neglected. Those forces can be calculated using:

$$F_t = F_{ad} + F_{rr} + F_{cr} + F_{af} \quad (1)$$

$$F_{ad} = \frac{1}{2} \delta C_{ad} A v_a^2 \quad (2)$$

$$F_{rr} = C_{rr} m g \quad (3)$$

$$F_{af} = m a \quad (4)$$

Where  $\delta$  : front surface area of vehicle [ $m^2$ ]  
 $C_{ad}$  : coefficient aerodynamic drag  
 $v_a$  : relative vehicle speed with respect to air [ $m/s$ ]  
 $C_{rr}$  : coefficient rolling resistance  
 $m$  : total vehicle mass, include the driver [ $kg$ ]  
 $g$  : gravitational acceleration [ $m/s^2$ ]  
 $a$  : acceleration [ $m/s^2$ ]

Calculation of the torque generated by the electric motor is based on energy considerations in terms of inertias ( $J$ ), load acceleration, coupling ratio ( $B$ ), and the load torque ( $T_L$ ) or force as shown below:

$$T_r = J \frac{d\omega_r}{dt} + B\omega_r + T_L \quad (5)$$

The losses in this model are neglected. The parameters of vehicle dynamics for a small electric karting can be seen in Table I.

TABLE I  
VEHICLE DYNAMIC PARAMETER FOR SMALL GO KART

Total mass	110	kg
Rolling resistance coeff.	0.03	
Drag coefficient	0.6	
Air density	1.202	kg/m <sup>3</sup>
Vehicle cross section	0.5	m <sup>2</sup>
Driving wheel radius	0.14	m

#### B. Electric Motor Losses

The losses in the electric motor can be divided into 4 components [12]: copper losses, core losses, mechanical losses and stray losses. In this paper, only copper and iron losses will be used in simulation and analysis. Mechanical and stray losses are disregarded. The electric motor that used in this paper is induction motor due to its simplicity, minimum maintenance requirement, and low costs [13]-[15].

Per-phase equivalent circuit of the induction motor at steady state is shown in Fig. 2 [15]-[18].

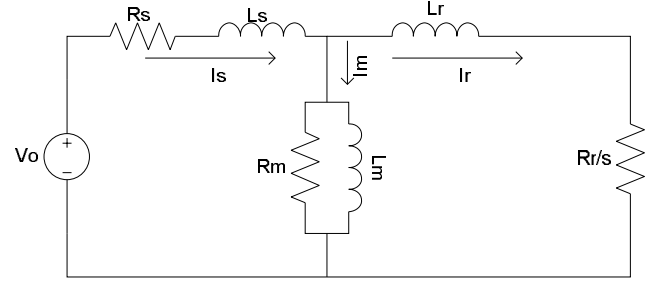


Fig. 2 Equivalent circuit of induction motor

From the equivalent circuit in Fig. 2 and power flow in induction motor, the rotor current at rated condition can be calculated by

$$I_r = \sqrt{\frac{2T_d \omega_s s}{3pR_r}} \quad (6)$$

Where  $T_d$  : developed torque of electric motor [T]  
 $s$  : slip [%]  
 $p$  : pole pairs  
 $\omega_s$  : angular speed of stator [rad/sec]

Using the current divider laws, the stator current is calculated by

$$V_g = \sqrt{\frac{s\omega_s T_d}{3R_r} \left( \frac{R_r^2}{s^2} + \omega_s^2 L_r^2 \right)} \quad (8)$$

Then the air gaps voltage can be expressed as

The total rated losses of the induction motor can be obtained as

$$P_{loss} = 3 \left[ R_s I_s^2 + R_r I_r^2 + \frac{V_g^2}{R_m} \right] \quad (9)$$

The induction motor can operate above the rated speed by using frequency or voltage control variations because of its rugged mechanical construction [10], [18]-[21].

The rating of the induction motor used in this paper can be seen in Table II.

TABLE II  
INDUCTION MOTOR RATING

Power	6000	W
Voltage	3 x 27	V
Frequency	100	Hz
Speed	2850	rpm
Current	168	A
Weight	19.2	kg

From this rating, the induction motor efficiency map can be calculated and the result can be seen in Fig. 3. Above the rated speed, the voltage is limited. Therefore, the power is constant and torque is varying. Below the rated speed, the current is limited at rated torque. Therefore, the voltage and frequency were adjusted to give the constant maximum torque.

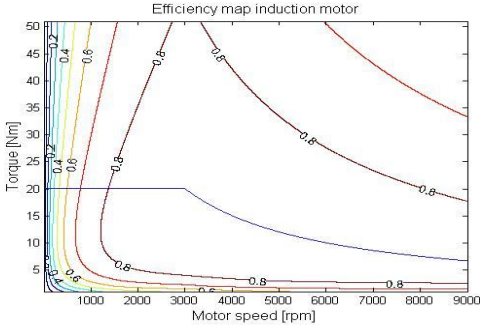


Fig. 3 Efficiency maps for the used induction motor

### C. Power Electronic Converter

The power electronic converter used in this simulation is a standard six-switch three-phase bridge inverter. The aim of this component is to provide appropriate mean values of parameters commonly used in electric motor. The power electronic component as power switching device used in this paper is MOSFETs (*Metal Oxide Semiconductor Field Effect transistors*) or IGBTs (*Insulated Gate Bipolar Transistors*) and anti-parallel power diodes. The controller pulse used in this simulation is a three-phase *pulse-width modulation* (PWM). The main losses in the converter are the conduction losses ( $P_{cond}$ ) and switching losses ( $P_{sw}$ ) for each switching component [10],[19]. Switching process of power electronic components depends on the load and switching strategies [19],[21]-[25].

The total losses for the MOSFET and IGBT are

$$P_Q = 6 \left[ \left( \frac{1}{8} + \frac{M}{3\pi} \cos(\theta) \right) R_{CE,on} I_Q^2 + \left( \frac{1}{2\pi} + \frac{M}{8} \cos(\theta) \right) I_Q V_{CE} + \frac{V_Q I_Q}{2} f_{sw} (t_{on,sw} + t_{off,sw}) \right] \quad (10)$$

where  $M$ : Modulation index ( $0 < M < 1$ )

$V_{CE}$  : collector-emitter voltage [V]

The losses for anti parallel power diode are almost the same with the losses in the MOSFET, except that the duty cycle of the anti parallel power diode is different due to different times of their operation. Also, the most important parameter in the diode switching losses is the reverse recovery losses. Therefore, the losses for the diode can be expressed by

$$P_D = 6 \left[ \left( \frac{1}{8} - \frac{M}{3\pi} \cos(\theta) \right) R_{D,on} I_D^2 + \left( \frac{1}{2\pi} - \frac{M}{8} \cos(\theta) \right) I_D V_D + \frac{f_{sw} V_R}{2S} \left( \frac{dI_F}{dt} \right) \left( \frac{St_{rr}}{S+1} \right)^2 \right] \quad (11)$$

The parameters of the power electronic converter block can be found in Table III.

TABLE III  
POWER ELECTRONIC CONVERTER PARAMETER

Power MOSFET MTD3055VL		
Strain drain to source on-resistance	0.012	ohm
Rise time	85e-9	seconds
Fall time	43e-9	seconds
Constant voltage drop	0	V
Power Diode QuietIR series 20 ETF		
Forward voltage drop	1.2	V
On-resistance	0	ohm
rms reverse voltage	21	V
Snappiness factor	0.6	
Rate of fall forward current	100e6	A/s
Reverse recovery time	60e-9	seconds
Controller		
Frequency switching	10	kHz
Modulation index	0.5	
Power factor motor	0.8	

### D. Battery

A battery is a device that converts chemical energy into electrical energy and vice versa. In this paper, a generic battery model will be used. The model is a modification of the Sheppard discharge battery model introduced by [26]. The battery is modeled using a controlled voltage source in series with constant internal resistance.

This model can represent the behavior of different battery types. The parameters of this model can be extracted from the discharge curve data or datasheet from the manufacturer. This model is based on several assumptions: the model has the same characteristic of charge and discharge cycles, the model has constant internal resistance and there is no-Peukert effect; the battery capacity does not change with the amplitude of the current.

The internal resistance battery (NiMH *Nilar Membrane Battery*) that will be used in the simulation is  $0.09\Omega$ . This value was got from the extraction of discharge curve of battery from manufacturer. The simulation used eight batteries as energy storage with the capacity was 36 Ah. The equivalent internal resistance of the total eight batteries was  $0.045\Omega$ .

### E. Regenerative Braking

Regenerative braking is a mechanism to reduce the vehicle speed by converting some of its kinetic energy to other useful form of energy [27]-[29]. This converted energy can be used to charge the energy storage in the system, such as a battery or a capacitor. The regenerative braking is different from an auxiliary drive braking, where the electrical energy is dissipated as heat by passing current through large bank of variable resistors.

Regenerative braking does not have a sufficient effect in

lowering the speed. Therefore, a friction brake is still required as complete brake and back-up brake. The total energy dissipation is limited by either the capacity of the supply system to absorb this energy or by the SOC of the battery. If SOC of the battery is full, the auxiliary drive braking will absorb the excess energy. In regenerative braking, the electric motor acts as generator and transfers the energy to the energy storage which provides braking effect. In order to capture the regenerative braking energy, the total traction torque must be negative.

### III. LOAD PROFILE OF THE ELECTRIC DRIVE SYSTEMS

The load used in this paper was drive cycle of ICE karting at race day for one lap (48 seconds). This drive cycle had previously been measured by the *Flap track* software at Göteborg karting ring track. The speed profile of the ICE karting for one lap can be seen in Fig. 4. The drive shall be optimized for 10 minutes heat in full race and 3 minutes for in and out laps.

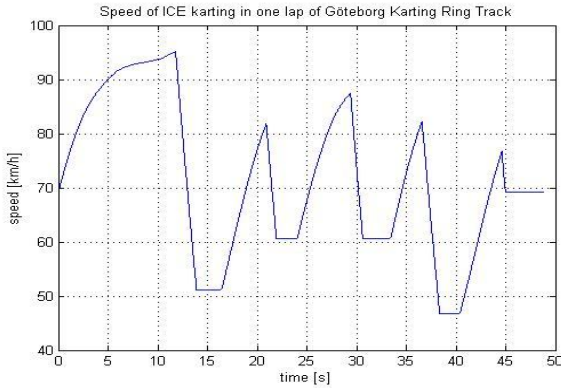


Fig. 4. Speed profile of ICE karting at Göteborg karting ring track

According to this speed characteristic, the traction torque at the wheel is varying between 47 Nm and -78 Nm. The negative torque indicates that the ICE karting is in deceleration or in regenerative braking region. It is clear that the regenerative braking or deceleration torque is higher than the acceleration torque. Therefore, the regenerative power used in charging the battery must be limited due to the limitation of the electric motor, power electronic converter and battery capability [27].

### IV. MODELING OF THE ELECTRIC DRIVE SYSTEM

The model of electric traction drive system for electric karting is implemented using Matlab®/Simulink® software. A steady-state model is used to get raw data that is helpful during the design stage and for long-term analysis over an extended drive cycle. The advantage of this modeling is fast computation. The steady-state model is suitable to model the efficiency and performance of the system.

The algorithm of the system can be seen in the flowchart in Fig.5. The reference load was used to calculate stator currents, rotor currents and air gap voltages of the electric motor. The stator and rotor currents were used to detect the normal or regenerative condition because the load torque was assumed to

be almost proportional to the currents. The currents were used to find the copper losses and the developed power in the electric motor, and the losses in the power electronic converter. The speed was also calculated based on developed torque. The efficiencies for normal and regenerative conditions were calculated using different formulas. Finally, the performance of the complete drive system was calculated and displayed.

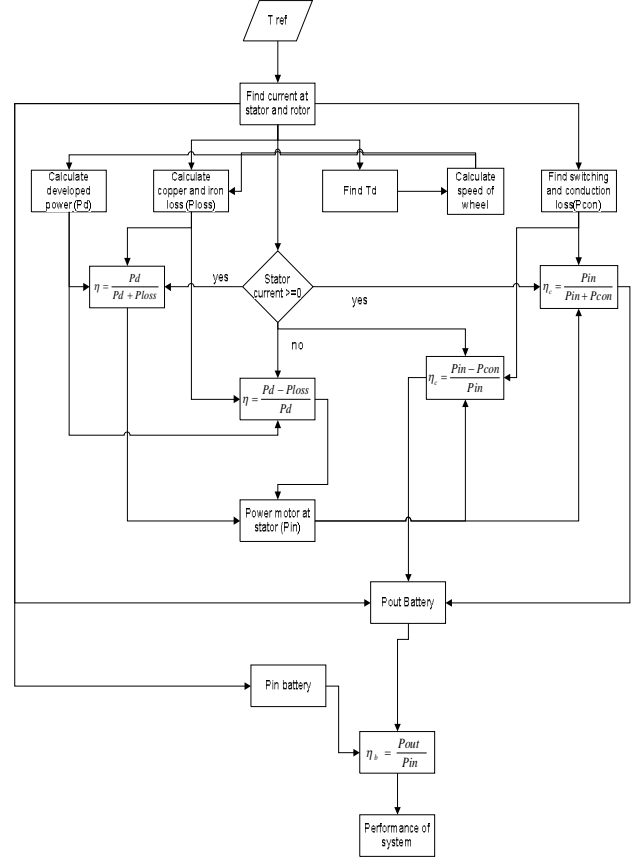


Fig. 5. Flowchart of the electric traction drive system algorithm

This simulation ran in 48 seconds and used variable-step ode45 (Dormant-Prince) solver. The relative tolerance was  $1e-3$ . There were also three *m files* that each represents the system parameters, displays the post processing, and includes calculation on the performance of each component of the system.

### V. RESULT AND DISCUSSION

According to the data sheet of the electric motor, the rated of the motor is 2850 rpm, 6000 W and 20.1 Nm. The speed and torque at the wheel were between 886 - 1801 rpm and 0 - 47 Nm respectively, as explained. This speed and torque must be geared to values that have a high efficiency of the electric motor. By using, the gear ratio used in this drive system has been selected to 45/21. With this gear ratio, the induction motor operates at speeds between 1889 - 3859 rpm and torques between 0 - 21.9 Nm. The slip of the induction motor was assumed to be constant because the electric motor operates

almost in the torque constant region. The mechanical losses of the electric motor and the vehicle dynamic model were assumed to be zero.

The average efficiency of the electric motor was 86.2%. The average efficiencies of the power electronic converter and the battery were 92.7% and 83.5%, respectively as seen in Fig. 6. Thus, the total average efficiency of this system was 66.7%. The lower efficiency at the battery occurred as a result of the large current in the equivalent internal resistance of the battery. At regenerative braking condition, the efficiency of the electric drive system was lower than that of normal operation due to the larger current in regenerative braking. Therefore, at regenerative braking condition, the losses increased in the power electronic converter, battery and electric motor.

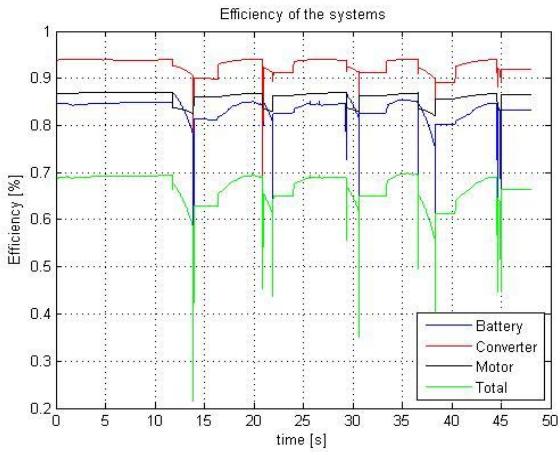


Fig. 6. Efficiency of the electric traction drive system for electric karting application using the induction motor.

The total energy used by the drive system is the subtraction of the regenerative energy from the used driving energy. The regenerative braking supplies a higher energy level in short time compared to normal operation. Consequently, this energy must be considered in designing an electric traction drive system. The total energy for 48 seconds at the electric motor in this drive cycle without regenerative braking was 53.5 Wh. The regenerative braking energy at the electric motor in this drive cycle was 15 Wh. As a result, the total energy of the electric motor with regenerative braking was 38.5 Wh. The total energy consumed by this electric traction drive system was 67.9 Wh, if the electric traction drive was run without using the regenerative braking energy. The total energy used by the electric traction drive system is 56.6 Wh with the regenerative braking energy supplying the energy (11.4 Wh) to the energy storage that can be seen in Table IV.

TABLE IV  
COMPARISON OF ENERGY USAGE

	Reg. [Wh]	W/o reg[Wh]		With reg[Wh]	
		a lap	13 min	a lap	13 min
Transmission	18.8	48.7	796.3	30.2	490.8
Motor	15	53.5	869.4	38.5	626.2
PEC	13.7	57.2	929.4	42	706.1
Battery	11.4	67.9	1104.5	56.6	920

Table IV shows that the total regenerative energy at the battery is lower than the total regenerative braking energy at the

electric motor due to losses at the components of the electric drive system.

The energy needed to operate the electric karting for 13 minutes was 920 Wh with regenerative braking, or 1104.5 Wh without regenerative braking. Therefore, the energy available in the battery (48Vdc) must be at minimum 19.2 Ah without regenerative braking, and 23 Ah with regenerative braking.

The performance of the battery in the electric traction drive system can be evaluated using the SOC of the battery during the drive cycle. The SOC of the battery can be seen in Fig. 7. At the end of simulation, the SOC of the battery was 0.9639. If the drive cycle is assumed to be the same for other times, the storage energy can support the electric traction drive system for 22 minutes and 51 seconds.

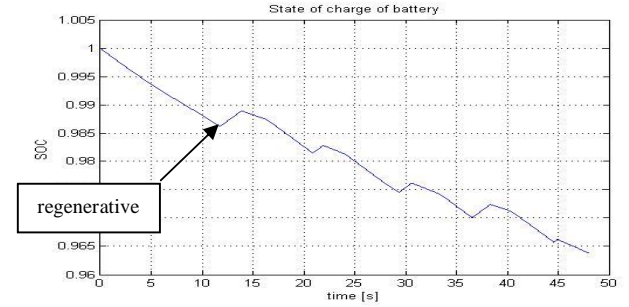


Fig. 7 State of charge of battery at electric traction drive system for electric karting application using induction motor

It is clear that the regenerative braking energy can be used to charge the battery and reduce the energy usage in the system.

A power and torque characteristics as function of the speed can be seen in Fig. 8. The transmitted power in the electric traction drive cycle increases with the increasing speed due to increasing frequency and voltage until the rated speed. The maximum power occurs in the rated speed. At above the rated speed, the transmitted power decreases again as a result of the decreasing stator and rotor currents. The torque is almost constant at rated torque below the rated speed and will decrease at above the rated speed due to decreasing power transmitted in the electric karting. At regenerative braking condition, the torque is almost constant above the rated torque of the electric motor.

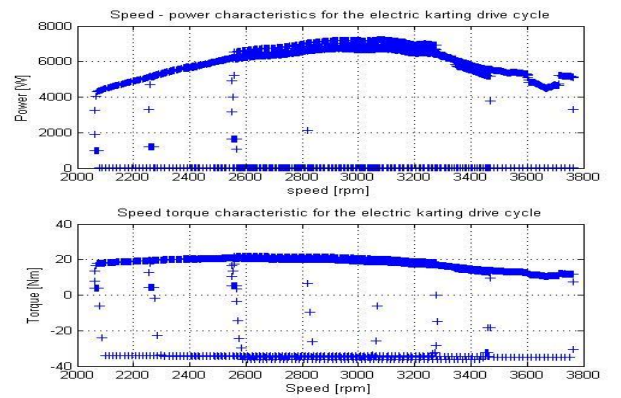


Fig. 8 Speed – power and torque characteristics of the electric karting using the induction motor drive system



## VI. CONCLUSION

The complete electric traction drive system was simulated and observed. The total average efficiency of the system was 66.7% and the total efficiency depended on the efficiency of the electric motor and the battery. In this simulation, there was no limitation for regenerative braking energy feed into the electric motor. The average power of the electric motor was found to be 5.4 kW. The total energy consumed for this electric traction drive system was 56.61 Wh in one lap with the regenerative braking energy and 920 Wh in the whole race.

From the case study analysis, the performance of the battery in the electric traction drive system can support the electric traction drive system for 22 minutes and 51 seconds. The type of battery can be changed to other types of battery which have a lower internal resistance but the price will be higher. It is clear that the regenerative braking energy can be used to charge the battery and reduce the energy usage in the system.

In this paper, the main focus has been placed on the induction motor modeling using the efficiency model on steady state. Thus, there exists much future research scope in improving the behavior of the electric motor, power electronic converter, and battery for dynamics simulation. Furthermore, the use of an advanced traction motor such as the permanent magnet DC motor, permanent magnet synchronous motor, series DC motor, brushless DC motor, and switched reluctance motor, which have even higher efficiencies, might lead to higher system efficiencies.

## VII. ACKNOWLEDGMENT

The authors gratefully acknowledge the contributions of Prof. Torbjörn Thiringer, Anders Lindskog, and Stig Ekstrom for their help, support, and guidance during this project.

## VIII. REFERENCES

- [1] J. Larminie, J. Lowry, *Electric Vehicle Technology Explained*, John Wiley and Sons, 2003
- [2] C. C. Chen, "An overview of electric vehicle technology," *Proceeding of IEEE*, vol. 81, no. 9, pp. 1202-1213, Sept 1993.
- [3] M. Ehsani, K. M. Rahman, H. A. Toliyat, "Propulsion system design of electric and hybrid vehicles," *IEEE TRANSACTIONS ON INDUSTRIAL ELECTRONICS*, VOL. 44, NO. 1, pp. 19-27, FEBRUARY 1997
- [4] [http://en.wikipedia.org/wiki/Go\\_karting](http://en.wikipedia.org/wiki/Go_karting) last visited 25 February 2009
- [5] [http://www.kartelec.com/f/en\\_actu.htm](http://www.kartelec.com/f/en_actu.htm) last visited 25 Februari 2009
- [6] C. Cardoso, J. Ferriera, V. Alves, R. E. Araujo, "The design and implementation of an electric go-kart for education in motor control," *IEEE International Symposium on Power Electronics, Electrical Drives, Automation, and Motion SPEEDAM 2006*, pp. 1489 – 1494, May 2006.
- [7] F. J. Perez-Pinal, C. Nunez, R. Alvarez, M. Gallegos, "Step by step design procedure of an independent-wheeled small EV applying EVLS," *IECON 2006-32<sup>nd</sup> Annual Conference on IEEE Industrial Electronics*, pp. 1176-1181, Nov 2006.
- [8] M. Xianmin, "Propulsion system control and simulation of electric vehicle in MATLAB software environment," *Proceeding of the 4<sup>th</sup> World Congress on Intelligent Control and Automation 2002*, pp. 815-818, June 2002.
- [9] J. M. Lee, B. H. Co, "Modeling and simulation of electric Vehicle power system," *Proceeding of the 32<sup>nd</sup> Intersociety IECEC-97*, vol. 3, pp. 2005-2010, August 1997
- [10] S.S. Williamson, A. Emadi, K. Rajashekara, "Comprehensive Efficiency Modeling of Electric Traction Motor Drives for Hybrid Electric Vehicles Propulsion Applications," *IEEE Transaction on Vehicular Technology*, vol. 56, no. 4, pp.1561-1572, July 2007.
- [11] Robert Bosch GmbH, *BOSCH-Automotive Handbook*, Robert Bosch GmbH, German, 2002
- [12] G. C. D. Sousa, B. K. Bose, "Loss modeling of converter induction machine system for variable speed drive," *Proceeding of the 1992 International Conference on Power electronics and Motion Control*, vol. 1, pp. 114-120, Nov. 1992
- [13] Mohamed A. El-Sharkawi, "Fundamentals of Electric Drives," *Brooks/Cole Thomson Learning*, 2000.
- [14] J.J. Cathey, "Electric Machines Analysis and Design Applying Matlab®," *McGraw Hill*, 2001
- [15] C. Shumei, L. Cheng, S. Liwei, "Study on Efficiency Calculation Model of Induction Motors for Electric Vehicles," *IEEE Vehicle Power and Propulsion Conference*, pp. 1-5, Sept 2008
- [16] J. Faiz, M. B. B. Sharifian, "Optimal design of an induction motor for an electric vehicle," *Euro. Trans. Electr. Power 2006*, vol. 16, pp. 15-33, July 2005.
- [17] G. Pugsley, C. Chillet, A. Fonseca, A-L. Bui-Van, "New modeling methodology for induction machine efficiency mapping for hybrid vehicles," *IEEE International Electric Machines and Drives Conference 2003*, vol.2, pp. 776-781, June 2003.
- [18] S.M. Lukic, A. Emado, "Modeling of Electric Machines for Automotive Applications Using Efficiency Maps," *Electrical Insulation Conference and Electrical Manufacturing & Coil Winding Technology Conference 2003*, pp. 543-550, Sept. 2003.
- [19] N. Mohan, T. M. undeland, and W. P. Robbins, "Power Electronics: Converter, Applications, and Design," Hoboken, NJ:Wiley, Oct 2002
- [20] B.K. Bose, "Power Electronics and Variable Frequency Drives," IEEE Press, New York, 1997.
- [21] B.K. Bose, "Modern Power Electronics and AC Drives," Prentice Hall, New York, 2002.
- [22] I. Husain, M. S. Islam, "Design, Modeling and Simulation of an Electric Vehicle System," *SAE-Advanced in Electric Vehicle Technology*, 1999-01-1149, March 1999.
- [23] Ali Emadi, "Handbook of Automotive Power Electronics and Motor Drives," *CRC Press – Taylor and Francis Groups*, Florida 2005
- [24] F. Casanellas, "Losses in PWM inverter using IGBTs," *IEE Proc. Electr. Power Appl.*, vol. 141, no. 5, pp. 235-239, September 1994.
- [25] P.A. Dahono, Y. Sato, T. Kataoka, "Analysis of conduction losses in inverter," *IEE Proc. Electr. Power Appl.*, vol. 142, no. 4, pp. 225-232, July 1995
- [26] O. Tremblay, L-A. Dessaint, A-I. Dekkiche, "A generic battery model for the dynamic simulation of hybrid electric vehicles," *IEEE Conference on Vehicles Power and Propulsion VPPC 2007*, pp. 284-289, Sept. 2007.
- [27] J. Lee, D. J. Nelson, "Rotating inertia impact on propulsion and regenerative braking for electric motor driven vehicles," *IEEE conference on Vehicle Power and Propulsion 2005*, pp. 308-314, Sept 2005.
- [28] B. Cao, Z. Bai, W. Zhang, "Research on control for regenerative braking of electric vehicle," *IEEE International Conference on Vehicular Electronics and Safety 2005*, pp. 92-97, Oct 2005.
- [29] Z. Junzhi, L. Xin, C. Shanglou, Z. Pengjun, "Coordinated control for regenerative braking system," *IEEE Vehicle Power and Propulsion Conference (VPPC)*, pp 1-6, Oct. 2008